Millimeter-Wave Power-Fading Compensation for WDM Fiber-Radio Transmission Using a Wavelength-Self-Tunable Single-Sideband Filter

Eric Vourc'h, Bernard Della, Denis Le Berre, and Didier Hervé

***Abstract*—Optical single-sideband (OSSB) sources compensate for deleterious chromatic dispersion effects in fiber-radio systems. We utilize the photorefractive properties of iron-doped indium phosphide (InP : Fe) to allow microwave–photonic interactions and design wavelength-independent OSSB filtering. Therefore, a wavelength-self-tunable single-sideband filter is built and characterized up to the millimeter-wave (31.5 GHz) domain. Compensation for fiber-dispersion penalties is achieved, showing photodetected power fluctuation along the fiber as low as 1 dB. In addition, we demonstrate the wavelength-division-multiplexing fiber-radio transmission of two OSSB channels transporting 140-Mbit/s binary phase-shift keying data at a 16 GHz RF over a 14-km fiber length followed by a 3-m radio link.**

***Index Terms*—Bragg grating, chromatic dispersion, hybrid fiber radio (HFR), iron-doped indium phosphide, optical double-sideband signal (ODSB), optical single-sideband signal (OSSB), photorefractive effect, wavelength division multiplexing (WDM).**

I. Introduction

HYBRID fiber-radio (HFR) architectures are an attractive solution for broad-band access since they allow quick and cost-effective network deployment [1], [2]. In HFR systems, a central office (CO) transmits optical carriers modulated at RF. The transmitted signals then propagate over fiber links toward remote base stations (BSs). At these locations, a photodiode (PD) converts the optical signal into an electrical RF signal, which is then amplified and transmitted by an antenna. Finally, the broad-band services are delivered to the customer by a radio link. Moreover, by also incorporating wavelength division multiplexing (WDM) techniques into the fiber access network, each BS can be addressed by a different wavelength. Such signal routing allows the number of services delivered to be increased and enables progressive deployment of the network [3].

Nevertheless, the standard amplitude modulation of optical carriers generates double-sideband (DSB) signals. Thus, due to the chromatic dispersion effects, each optical line propagates in the fiber at a different speed. Consequently, on arrival at the BS, the sidebands are phase shifted. Since the BS's PD is a quadratic detector, the recovered power level P_{RF} is a function of the phase shift [see (1)]. Thus, P_{RF} suffers from periodical fading depending on the fiber length L and on the square of the modulation frequency f_m [see (2)] [4]

$$\Phi = \frac{\pi L D \lambda^2 f_m^2}{c} \tag{1}$$

$$P_{\mathrm{RF}} \propto \cos^2\left(\frac{\pi L D \lambda^2 f_m^2}{c}\right). \tag{2}$$

In the above equations, c is the velocity of light, λ is the optical carrier wavelength, and D is the fiber-dispersion parameter. Moreover, problems associated with chromatic dispersion are aggravated since the distance where the first fading occurs varies with the optical modulator's chirp parameter.

The power fading drawback is eliminated when a single-sideband (SSB) signal is used as reported in recent research focusing on fiber-wireless issues [5], [6]. Optical single-sideband (OSSB) generation has previously been achieved using the double modulation of a dual-electrode Mach–Zehnder modulator (MZM) [7] biased at quadrature or using a source integrating two electro-absorption modulators (EAM) [8]. Another effective solution relies on the suppression of one of the sidebands of a DSB signal by means of a fixed Bragg grating [9]. In the same manner, configurations implementing a mechanically tuned Bragg grating [10] or a tapered linearly chirped fiber grating [11] have also led to power-fading compensation. However, despite their simplicity, the latter filtering techniques have the disadvantage of being dependent on the wavelength of the optical carrier. In our approach, we utilize the photorefractive effect in an iron-doped indium phosphide (InP : Fe) crystal to generate an OSSB signal. The principle of the device is to take a part of an optical double-sideband (ODSB) signal to generate three dynamic Bragg gratings inside the bulk crystal via the photorefractive effect [12]. Simultaneously, the second part of the ODSB signal is injected into the gratings under the appropriate Bragg angle whose value is dictated by the modulation frequency f_m. In this way, two Bragg conditions are reached that lead to the diffraction of an OSSB signal made up of the carrier and the lower sideband of the input signal. In addition, since the input ODSB signal drives the dynamic Bragg gratings induced inside the crystal, the device is wavelength-self-tunable (WST) [13].

Manuscript received April 5, 2002; revised July 22, 2002.

The authors are with the Laboratoire d'Electronique et des Systèmes de Télécommunications Unité Mixte de Recherche du Centre National de la Recherche Scientifique 6165, Ecole Nationale Supérieure des Télécommunications de Bretagne (ENST-Bretagne), 29285 Brest Cedex, France (e-mail: eric.vourch@enst-bretagne.fr).

Digital Object Identifier 10.1109/TMTT.2002.805167

In Section II of this paper, we report on the principle of the wavelength-self-tunable single-sideband (WST-SSB) filter, and we describe the experimental setup of the device. Section III reports the millimeter-wave characterization of a WST-SSB filter: first, output spectra corresponding to 31.5-GHz modulated input signals are measured and discussed. Second, we present a chromatic dispersion compensation experiment again performed at 31.5 GHz, showing less than 1-dB detected RF power fluctuation. In Section IV, a WDM fiber-radio system experiment implementing a WST-SSB filter is demonstrated. The system RF was 16 GHz and was binary phase-shift keyed with a 140-Mbit/s data stream. Two optical SSB signals were transmitted over a 14-km fiber length before one channel was photodetected and subsequently radio-transmitted over a 3-m distance. Finally, the eye pattern of the down-converted received signal was observed.

II. WST-SSB Filter Concept and Experimental Setup

A. WST-SSB Concept

A photorefractive material is an electrooptic crystal in which light illumination generates free carriers. InP : Fe belongs to this category and is particularly interesting since it reacts to the 1.55-μm wavelengths used for optical-fiber telecommunications [14]. Therefore, a control beam in this wavelength range can be used to generate a Bragg grating inside an InP : Fe crystal. In fact, thanks to a simple interference pattern, the photorefractive effect leads to a periodic variation of the refractive index. First, the counter propagative illumination of an InP : Fe bulk crystal is obtained thanks to the control beam's reflection off a mirror placed behind the crystal. Thus, the interference pattern obtained results in a periodic illumination inside the crystal. The carrier generation and trapping then produce a periodic charge distribution. Finally, the electrooptic effect combined with the periodic electrical field due to the charge distribution generate a periodic refractive index. This Bragg grating makes it possible to diffract a signal beam of wavelength λ_s. According to the Bragg condition, the value of λ_s is linked to the grating period Λ, which, in our case, depends on the control beam wavelength λ_c [see (3)]. Equation (4) gives the relation between λ_s and λ_c. It is to be noted that λ_c is greater than λ_s

$$\Lambda = \frac{\lambda_c}{2n} \tag{3}$$

$$\lambda_s = \lambda_c \sqrt{1 - \left(\frac{\sin\theta}{n}\right)^2}. \tag{4}$$

In (3) and (4), n is the crystal average refractive index and θ is the angle separating the signal beam from the control beam outside the crystal. Obviously, the value we set θ at fixes the wavelength difference $\Delta\lambda$ between λ_s and λ_c. Consequently, regarding an optical DSB signal, θ can be set so that $\Delta\lambda$ coincides with the wavelength difference between the carrier and sidebands. Therefore, in this configuration (Fig. 1), we divide the DSB signal into two beams. The first one is used as the control beam and the second one as the signal beam. In this way, the three control lines ($\lambda_{1,2,3}$) generate three Bragg gratings ($G_{1,2,3}$). Then, according to the relation [see (4)] that exists between a control wavelength λ_i and a signal wavelength λ_{i-1}, G_2 and G_3 will diffract the signal lines λ_1 and λ_2, respectively. Thus, these diffracted carrier and lower sideband constitute an OSSB signal that is collected at the device output.

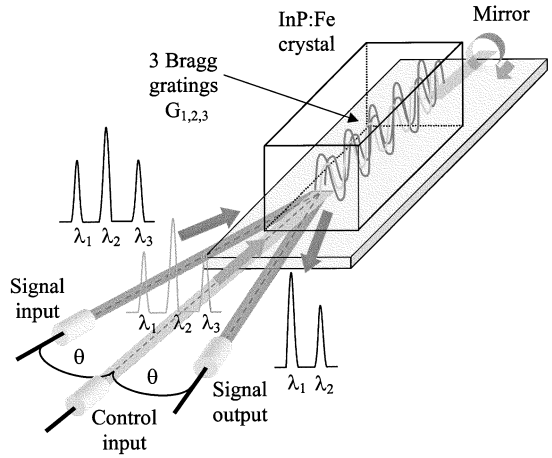

Fig. 1. WST-SSB filter concept.

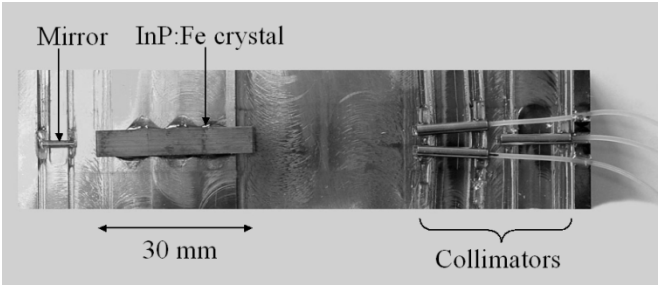

Fig. 2. WST-SSB filter built with a 30-mm-long InP : Fe bulk crystal.

In addition, θ being fixed, the filter works for a given modulation frequency f_m according to (5). The measured bandwidth of the device is in the order of 2 GHz [15], which allows 1-Gbit/s bit rates to be considered. This 3-dB bandwidth ($\mathrm{BW}_{3\,\mathrm{dB}}$) is linked to the bulk crystal's length by (6). Moreover, since the input DSB signal drives the filter, the latter is WST. This property is the main advantage of this technique with respect to integrated SSB modulation sources or other filtering techniques using fixed Bragg gratings

$$f_m \cong \frac{c\sin^2\theta}{2n^2\lambda_c} \tag{5}$$

$$\mathrm{BW}_{3\,\mathrm{dB}} \cong \frac{c}{2nL}. \tag{6}$$

B. WST-SSB Device Experimental Setup

Fig. 2 shows the way the WST-SSB filter was implemented for the subsequent experiments. The InP : Fe crystal used was 30-mm long with a mirror glued behind it in order to permit the control beam interference. The input and output accesses used collimators whose angles were placed by means of micropositioning systems. The angles were changed whenever the experiment needed a change in the device operating frequency.

Moreover, the InP : Fe physical parameters confer on the filter a few milliseconds response time, as well as a theoretical

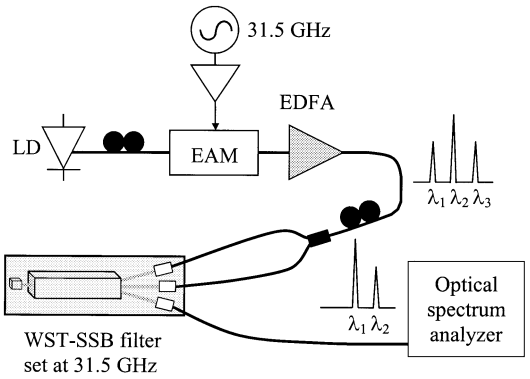

Fig. 3. Experimental setup for measuring the single-channel 31.5-GHz WST-SSB filter output spectrum.

fiber-to-fiber diffraction efficiency of approximately −20 dB (between the input and output signals in a configuration only implementing a single signal line and a single control line) [16]. The latter reflectivity will be examined in greater detail in Section III.

III. Characterization

A. WST-SSB Filter Output Spectra Measurements

In order to characterize the WST-SSB filter described in Section II, spectral response measurements were conducted in both the microwave and millimeter-wave frequency domains. Moreover, two experimental configurations were set up. First, the filter's output spectrum corresponding to one DSB signal at the input was observed. Second, the output signal was measured, while two DSB WDM channels were injected at the input. Results reported here were obtained for optical signals modulated at a 31.5-GHz RF.

In the single-channel experimental setup (Fig. 3), the optical carrier emitted by a 1.55-μm LD was injected into a multiquantum-well EAM, driven at 31.5 GHz with 9.5-dBm RF power applied. At this stage, an erbium-doped fiber amplifier (EDFA) was used in order to compensate for the 15.8-dB insertion loss in the modulator and provide a sufficient pump level for the gratings. The resulting DSB signal was fed through a polarization controller into a 3-dB optical coupler connected to the WST-SSB filters' inputs. Of course, the device's collimator angles were adjusted beforehand so that the operating frequency was 31.5 GHz. Finally, the diffracted signal was observed with an optical spectrum analyzer (OSA). The DSB input signal, which had a 8-dBm carrier level and a −3.5-dBm sideband level, is shown in Fig. 4(a). On the other hand, Fig. 4(b) shows the diffracted signal, which, as predicted in Section II, was SSB with an upper sideband rejection up to 39 dB. Nevertheless, it is to be noted that the diffracted lower sideband (λ_1) level is higher than the diffracted carrier (λ_2) level. This was predictable since grating G_2 is of higher amplitude than grating G_3, as they are generated by the optical carrier and upper sideband, respectively. In addition, the experiment implemented different laser diodes (LDs). In this way, we could verify that the SSB diffracted signal followed a carrier-wavelength change.

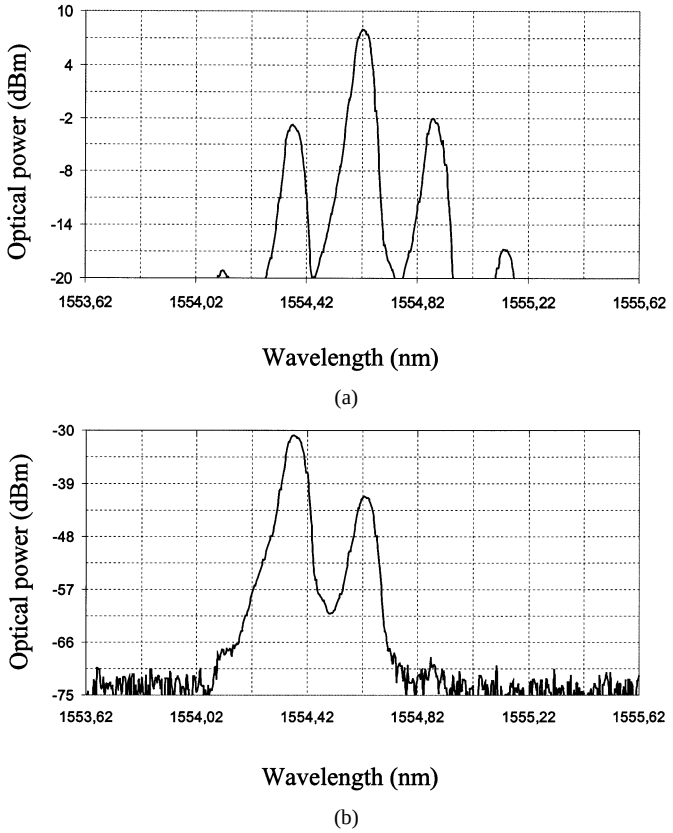

Fig. 4. Measured optical spectra in the 31.5-GHz single-channel WST-SSB filter characterization experiment. (a) Spectrum at the WST-SSB filter input. (b) Spectrum at the WST-SSB filter output.

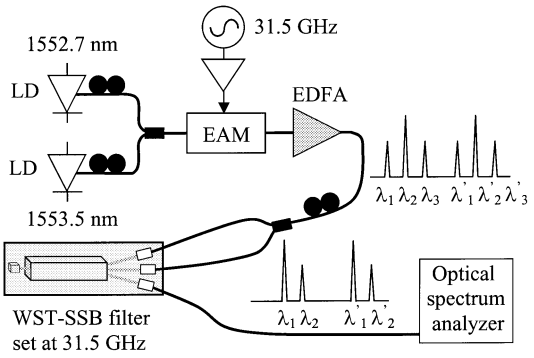

Fig. 5. Experimental setup for measuring the 31.5-GHz two-channel WST-SSB filter output spectrum.

Regarding the two WDM channel spectral response measurements (Fig. 5), two optical carriers were injected into the EAM. The RF driving of the modulator was again a 9.5-dBm signal at the 31.5-GHz frequency and the rest of the setup was also similar to the single-channel case. Nevertheless, in this new configuration, six dynamic Bragg gratings were assumed to be generated inside the InP : Fe crystal. As a consequence, in order to prevent misdiffraction of the first channel's upper sideband by the grating due to the second channel's lower sideband, the wavelengths of the carriers were spaced 0.8 nm apart. Fig. 6(a) and (b) shows the optical spectrum before the input coupler of the WST-SSB filter and the diffracted spectrum, respectively. Two SSB channels are obtained with a 30-dB upper sideband rejection.

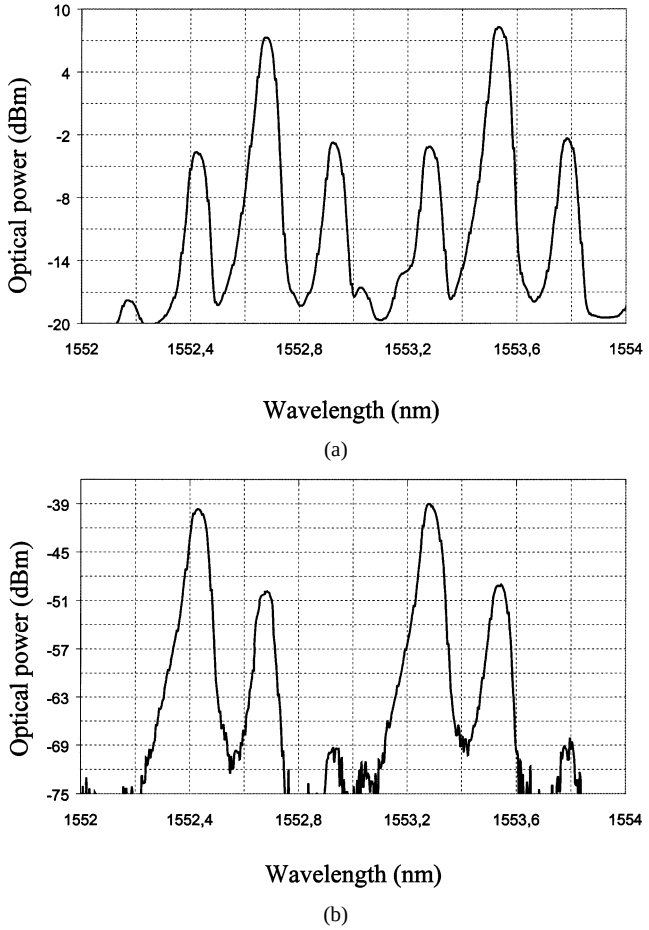

Fig. 6. Measured optical spectra in the 31.5-GHz two-WDM-channel WST-SSB filter characterization experiment. (a) Spectrum at the WST-SSB filter input. (b) Spectrum at the WST-SSB filter output.

Obviously, the low fiber-to-fiber efficiency is the characteristic to be improved in our experimentation. Indeed, in the one-channel case, the measured power level difference between the input and output lower sidebands is 28 dB. Nevertheless, the use of an efficient EAM with greater modulation depth (0.3 instead of the current lower than 0.1 value) would increase the input sideband levels and would consequently also increase the diffracted sideband level. Furthermore, in the two-WDM-channel case, the fiber-to-fiber efficiency decreases by 8 dB. This results from the fact that when a second channel is added, the Bragg grating modulation indexes are divided by two.

In comparison, cadmium telluride (CdTe) is another material that is also photorefractive in the 1.55-μm-wavelength range [17]. Theory predicts that the use of such a crystal could at least double the reflectivity thanks to its 5.5 pm $\cdot$ V^{-1} electrooptic coefficient [18] against 1.7 pm $\cdot$ V^{-1} for InP : Fe.

Nevertheless, from our point-of-view, InP : Fe seems a more promising choice since it allows InGaAsP integration of the device to be considered. Indeed, such an alternative could reduce the 4.5-dB loss due to the collimators. On the other hand, the filter's throughput could be increased by also integrating an optical semiconductor amplifier at the output of the device.

Furthermore, as far as polarization is concerned, we observed that a polarization controller could optimize the diffracted level. Nevertheless, this dependency is not an issue since the WST-SSB filter is a transmitter device.

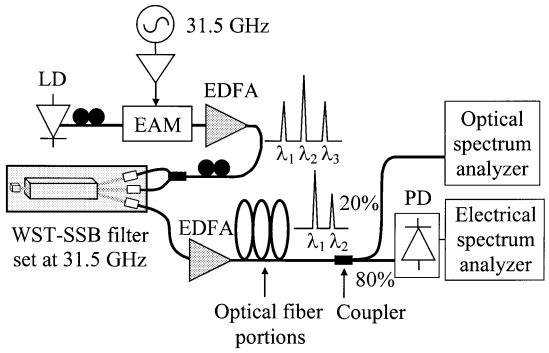

Fig. 7. Setup of the millimeter-wave (31.5 GHz) chromatic dispersion compensation experiment using the WST-SSB filter.

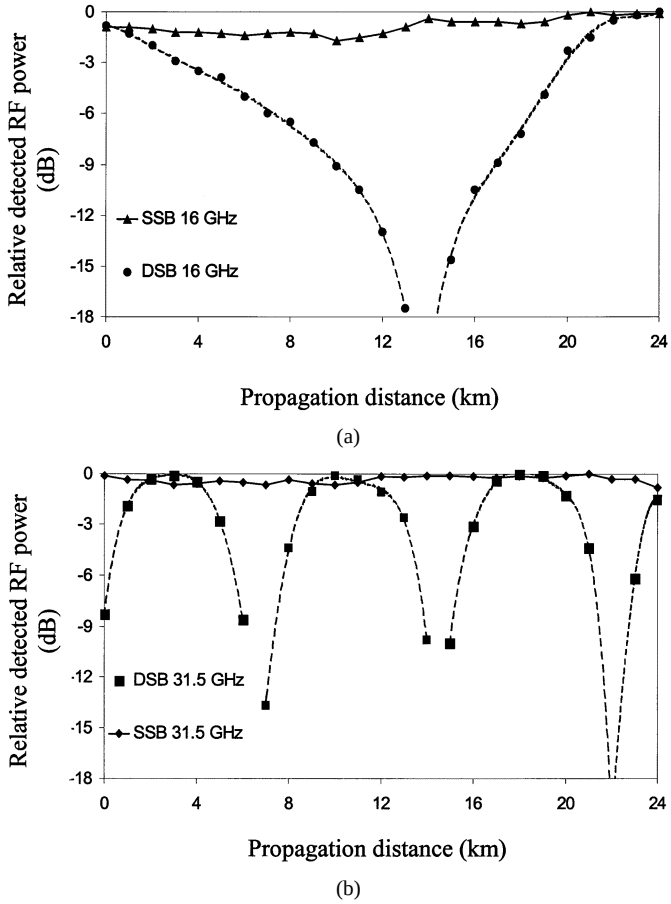

Fig. 8. Recovered electrical power levels as a function of fiber length for: (a) 16- and (b) 31.5-GHz modulated optical DSB signals and for SSB signals obtained using a WST-SSB filter.

In addition, we estimated that a 0.06° offset of the collimators' angles induced a central frequency shift of the filter in the order of 1 GHz. This value was evaluated by comparison between angles set for a 16- and 31.5-GHz filter operating frequency and it is in good agreement with theoretical predictions [see (5)].

B. Power-Fading Compensation Experiments

After preliminary spectral response observation, characterization was completed by measuring the detected power

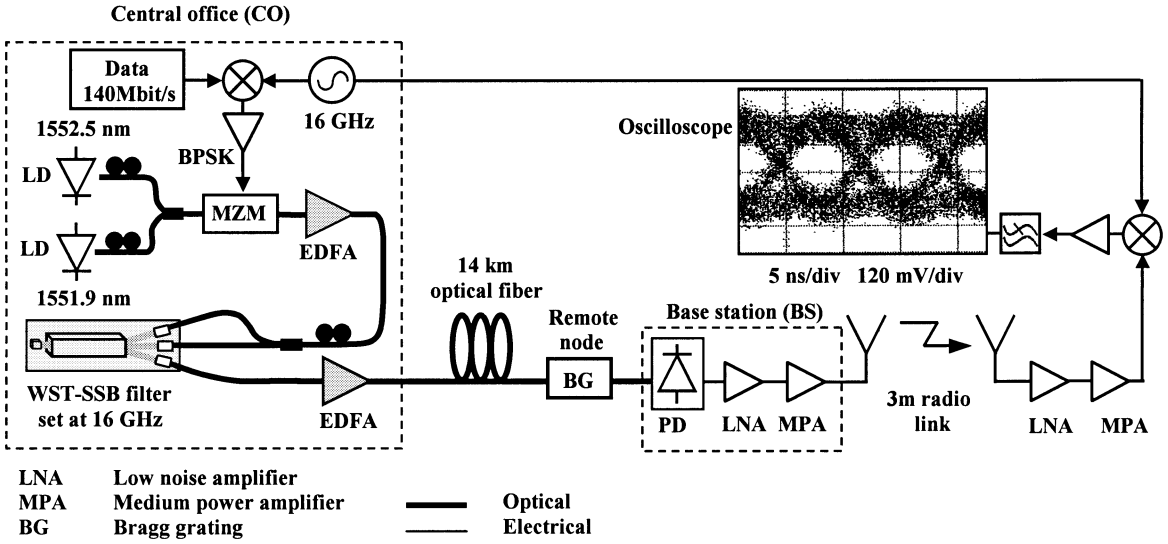

Fig. 9. Experimental setup of the system transmitting 140-Mbit/s data streams at 16-GHz RF, incorporating the WST-SSB filter. The demultiplexing and radio transmission of one channel follow the transmission of two WDM channels over a 14-km fiber link.

variations along the fiber using either ODSB or OSSB signals. For this purpose, the experiment depicted in Fig. 7 was implemented. An optical modulator, driven by an RF electrical signal, externally modulated an optical carrier emitted by an LD. The resulting DSB signal was amplified by an EDFA and injected into the WST-SSB filter inputs by means of a 3-dB optical coupler. At the output, the OSSB signal was also boosted by an EDFA and transmitted into fibers whose lengths varied up to 24 km. The first EDFA was necessary because of the insertion loss in the modulator, whereas the second one compensated for the filter low reflectivity and the loss in the fibers. In addition, a 80%/20% coupler was implemented at the fiber output. The 80% path was connected to the high-speed PD, while the 20% one was directed to an OSA so as to make sure a constant optical signal power level was injected into the PD. The recovered RF electrical signal was then measured at the electrical spectrum analyzer. First, the RF was chosen to be 16 GHz and an MZM was used. The latter device was then replaced by an EAM driven at a 31.5-GHz RF. Moreover, in each case, the WST-SSB filter operating frequency was set to the desired RF thanks to appropriate adjustment of the injection angle. Measurement results are plotted in Fig. 8, the dashed line and the solid curve representing power levels recovered with a DSB and SSB signal, respectively. Naturally, for ODSB signal propagation, measurements show higher than 20-dB fading of the photodetected power level. On the contrary, when a WST-SSB filter is used, no power fading is encountered and the maximum fluctuation attributable to a small remaining upper sideband level did not exceed 1 dB [see Fig. 8(a)] and 0.8 dB [see Fig. 8(b)] for the 16- and 31.5-GHz signals, respectively.

IV. WDM Fiber-Radio Experiment

Characterization experiments having confirmed the theoretical behavior of the device with respect to chromatic dispersion effects, a system implementation was necessary for further validation. With this aim in view, the WDM fiber-radio data transmission shown in Fig. 9 was carried out. The RF equipment

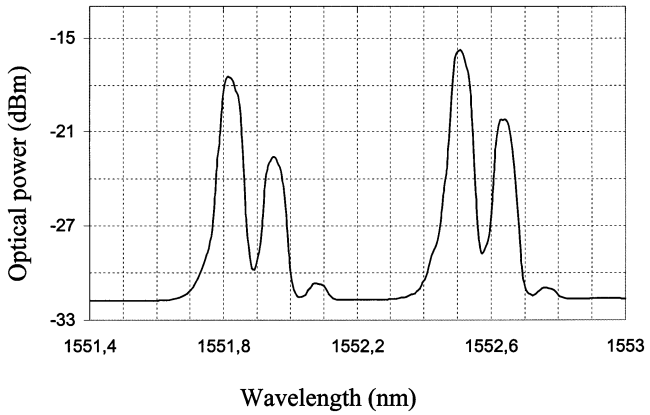

Fig. 10. Amplified WST-SSB output signal measured for a two-channel WDM input DSB signal with 16-GHz RF.

available led us to choose a 16-GHz carrier frequency. The transmitter implemented two tunable lasers whose emitted carriers were set at 1551.9 and 1552.5 nm, respectively. Each carrier was directed to one path of an optical coupler through a polarization controller and the coupler output was fed to an MZM. A 16-GHz RF carrier, binary phase-shift keyed by a 140-Mbit/s data stream (HP 3764A), was used to drive the MZM (RF electrode). Again to compensate for the MZM insertion loss and provide a sufficient pump level, the two optical DSB signals obtained at the MZM output were amplified by an EDFA before being fed to the optical coupler at the WST-SSB filter input. Prior to implementing a fiber-wireless transmission, the filter output spectrum was observed at the OSA. Fig. 10 shows the two boosted WDM-SSB channels. A 14-km fiber link was then added between the transmitter and a remote BS. At this location, a Bragg grating was used to suppress the WDM channel at 1551.9 nm. Next, the RF signal recovered from the remaining optical SSB signal was amplified and radio transmitted over a 3-m distance. Finally, after amplification, the received signal was down-converted and the eye pattern was observed. The clear eye opening (Fig. 9) proves the good quality of the data transmission. Nev-

ertheless, the latter could certainly be improved and noise could be reduced by the use of optimized RF amplifiers and optical filtering after the EDFA. However, the current system experiment demonstrates that a single WST-SSB filter can reach a dispersion-free two-channel WDM fiber-radio data transmission.

V. Conclusion

We have investigated the compensation of the chromatic dispersion effects in radio-over-fiber transmissions using a WST-SSB filter. The principle of the device relies on the photorefractive effect in an InP : Fe crystal. The ODSB signal to filter generates itself the dynamic Bragg gratings that diffract the carrier and lower sideband. Thus, the device operates independently of the carrier wavelength, whereas the operating frequency is set to the desired microwave or millimeter-wave value by simply adjusting the signal injection angle. A device has been built according to this concept, and then millimeter-wave characterization performed using 31.5-GHz modulated optical input signals has validated theoretical behavior. For instance, the observed fluctuation due to chromatic dispersion along the fiber was as low as 1 dB. However, due to the InP : Fe crystal's physical characteristics, the measured filter's fiber-to-fiber efficiency was in the order of -28 dB, which could be improved by using another crystal with enhanced physical characteristics. A new photorefractive material such as CdTe or InGaAsP integration that could include a semiconductor optical amplifier would certainly improve the device's reflectivity. Furthermore, a two-channel WDM fiber-radio system experiment incorporating the device has been demonstrated for the first time. The RF was 16 GHz and the eye diagram of the 140-Mbit/s data stream observed at the receiver after a 14-km optical transmission and a 3-m radio link was wide open.

Acknowledgment

The authors wish to acknowledge the assistance and support of France Telecom Research and Development Lannion, Lannion, France. The authors are particularly grateful to R. Coquillé, France Research and Telecom Research and Development Lannion, Lannion, France, for providing the InP : Fe crystals and to E. Pincemin, France Research and Telecom Research and Development Lannion, for his assistance regarding the high-speed devices. The authors would also like to thank Dr. E. Vergnol, France Telecom, Issy le Moulineaux, France, for helpful discussions, as well as Dr. J. Ormrod, Ecole Nationale Supérieure des Télécommunications (ENST)-Bretagne, Brest, France.

References

[1] J. R. Forrest, "Communication networks for the new millennium," *IEEE Trans. Microwave Theory Tech.*, vol. 47, pp. 2195–2201, Dec. 1999.

[2] K. Kitayama, "Architectural considerations of radio-on-fiber millimeter-wave wireless access systems," in *Proc. ISSSE*, 1998, pp. 378–383.

[3] A. Nirmalathas, C. Lim, D. Novak, D. Castleford, R. Waterhouse, and G. Smith, "Millimeter-wave fiber-wireless access systems incorporating wavelength division multiplexing," in *Proc. Asia–Pacific Microwave Conf.*, 2000, pp. 625–629.

[4] U. Gliese, S. Norskov, and T. N. Nielsen, "Chromatic dispersion in fiber-optic microwave and millimeter-wave links," *IEEE Trans. Microwave Theory Tech.*, vol. 44, pp. 1716–1724, Oct. 1996.

[5] A. Narasimha, X. Meng, C. F. Lam, M. C. Wu, and E. Yablonovitch, "Maximizing spectral utilization in WDM systems by microwave domain filtering of tandem single sidebands," *IEEE Trans. Microwave Theory Tech.*, vol. 49, pp. 2042–2047, Oct. 2001.

[6] A. Nirmalathas, D. Novak, C. Lim, and R. B. Waterhouse, "Wavelength reuse in the WDM optical interface of a millimeter-wave fiber-wireless antenna base station," *IEEE Trans. Microwave Theory Tech.*, vol. 49, pp. 2006–2012, Oct. 2001.

[7] G. H. Smith, D. Novak, and Z. Ahmed, "Overcoming chromatic-dispersion effects in fiber-wireless systems incorporating external modulators," *IEEE Trans. Microwave Theory Tech.*, vol. 45, pp. 1410–1415, Aug. 1997.

[8] E. Vergnol, F. Devaux, D. Tanguy, and E. Pénard, "Integrated lightwave millimetric single side-band source: Design and issues," *J. Lightwave Technol.*, vol. 16, pp. 1276–1284, July 1998.

[9] J. Park, W. V. Sorin, and K. Y. Lau, "Elimination of the fiber chromatic dispersion penalty on 1550 nm millimeter-wave optical transmission," *Electron. Lett.*, vol. 33, pp. 512–513, Mar. 1997.

[10] S. A. Havstad, A. B. Sahin, O. H. Adamczyk, Y. Xie, and A. E. Willner, "Distance-independent microwave and millimeter-wave power fading compensation using a phase diversity configuration," *IEEE Photon. Technol. Lett.*, vol. 12, pp. 1052–1054, Aug. 2000.

[11] J. Marti, J. M. Fuster, and R. I. Laming, "Experimental reduction of chromatic dispersion effects in lightwave microwave/millimeter-wave transmissions using tapered linearly chirped fiber gratings," *Electron. Lett.*, vol. 33, pp. 1170–1171, June 1997.

[12] E. Vourch, D. Le Berre, and D. Hervé, "Lightwave single-side-band source using a wavelength self-tunable InP : Fe filter for fiber-wireless systems," in *Proc. IEEE Int. Microwave Photon. Topical Meeting*, Long Beach, CA, 2002, pp. 199–202.

[13] ——, "Lightwave single-side-band wavelength self-tunable filter using an InP : Fe crystal for fiber-wireless systems," *IEEE Photon. Technol. Lett.*, vol. 14, pp. 194–196, Feb. 2002.

[14] A. M. Glass and J. Strait, "Photorefractive materials and their applications I," in *Topics in Applied Physics*, P. Gunter and J. P. Huignard, Eds. Berlin, Germany: Springer-Verlag, 1988, vol. 61, pp. 237–262.

[15] D. Hervé, J. F. Cadiou, R. Coquillé, and S. Pinel, "A novel photonic technique using a dynamic Bragg grating in InP : Fe for microwave modulation frequency control of fiber-wireless systems," in *Proc. IEEE Int. Microwave Photon. Topical Meeting*, Melbourne, Australia, 1999, pp. 227–230.

[16] D. Hervé, "Study of a tunable optical filter using the photorefractive effect in iron-doped indium phosphide with transposition to guided optics," Ph.D. dissertation (in French), Univ. Brest, Brest, France, 1996.

[17] J. Y. Moisan, N. Wolffer, O. Moine, P. Gravey, G. Martel, A. Aoudia, E. Repka, Y. Maifaing, and R. Tiboulet, "Characterization of photorefractive CdTe : V: High two-wave mixing gain with an optimum low-frequency periodic external electric field," *J. Opt. Soc. Amer. B, Opt. Phys.*, vol. 11, no. 9, pp. 1655–1667, Sept. 1994.

[18] G. Martel, "Study of the photorefractive effect in $Cd_{1-x}Zn_xTe$ and application to free space interconnection with double-phase-conjugate-mirror," Ph.D. dissertation (in French), Univ. Rouen, Rouen, France, 1996.

Eric Vourc'h was born in Brest, France, in 1974. He received the B.S. degree in physics and M.S. degree in electrical and electronic engineering from the University of Brest, Brest, France, in 1998 and 1999 respectively, and is currently working toward the Ph.D. degree in electronics at the Laboratory of Electronics and Telecommunication Systems (LEST), Brest, France, which is run jointly by the Ecole Nationale Supérieure des Télécommunications de Bretagne (ENST-Bretagne/French National School of Telecommunications Engineering of Brittany) and the University of Brest. His doctoral research concerns fiber-wireless communication systems.

From 1999 to 2002 he was a Part-Time Lecturer with the University of Brest.

Mr. Vourc'h was the recipient of the First Prize of the Student Paper Competition of the 2001 IEEE International Microwave Photonics Topical Meeting. He was also a recipient of the International Engineering Consortium's William L. Evritt Student Award of Excellence (IEC), Chicago, 2002.

Bernard Della was born in Brest, France, in 1952. In 1975 he passed the Entrance examination to France Telecom, Quimper, France.

From 1975 to 1977, he was a Staff Member with the Centre National d'Etude des Télécommunications, Paris, France, where he was involved with numerical switching cards. In 1978, he joined the Ecole Nationale Supérieure des Télécommunications de Bretagne (ENST-Bretagne/French National School of Telecommunications Engineering of Brittany), Brest, France, where he is currently a Member of the Technical Staff with the Microwave Department. His research activities concern the development of hybrid integration technologies for both RF and opto-electronic communication systems.

Denis Le Berre received the Ph.D. degree in electronics from the University of Brest, Brest, France, in 1997.

Since 1997, he has been an Associate Professor with the Electronics Department, University of Brest, where he currently performed research with the Laboratory of Electronics and Telecommunication Systems (LEST). His activities concern the design of microwave circuits for the impedance matching of opto-electronic components. His research interests also include optical devices and lightwave system modeling.

Didier Hervé was born in Treguier, France, in 1962. He received the B.S. degree in electrical and electronic engineering, and M.S. and Ph.D. degrees from the University of Brest, Brest, France, in 1984, 1992, and 1996, respectively. His doctoral research involved dynamic Bragg gratings in iron-doped indium phosphide, which led to the design of a new high-resolution OSA. His investigations also focused on photorefractive waveguide structures in III–V compounds. This work was carried out jointly with the France Telecom Research and Development Center, Lannion, France.

From 1985 to 1988, he was with France Telecom, Paris, France, as a Switching Exchange Technical Manager. In 1989, he joined the teaching staff of the Microwave Department, Ecole Nationale Supérieure des Télécommunications de Bretagne in Brest, France (ENST-Bretagne/French National School of Telecommunications Engineering of Brittany). In 1998, he was a Visiting Scholar with the University of Sydney, Sydney, Australia, where he was involved with a project including fiber Bragg gratings for optical signal-processing applications. His current research activities are focused on the microwave photonics field, particularly on hybrid fiber-wireless distribution systems. Since he was promoted Associate Professor in 1998, he has also been involved with the International Relations Division, ENST-Bretagne, for student-exchange programs, mainly with Australia and Spain.